



# Usefulness of PETRA-MRA for Postoperative Follow-Up of Stent-Assisted Coil Embolization of Cerebral Aneurysms

Yusuke Ebiko, Hikaru Wakabayashi, Tomoaki Okada, Tatsuya Mizoue, and Shinichi Wakabayashi

**Objective:** Image evaluation after stent-assisted coil embolization (SAC) for a cerebral aneurysm is difficult with conventional MRA or CTA because of metal artifacts. Pointwise encoding time reduction with radial acquisition (PETRA)-MRA is a noninvasive imaging examination that can reduce metal artifacts. This study aimed to examine whether PETRA-MRA can be used as a follow-up imaging after SAC.

**Methods:** Twelve patients (eight women and four men; mean age,  $66.9 \pm 13.2$  years) underwent SAC for unruptured aneurysms and were retrospectively evaluated using time-of-flight (TOF)- and PETRA-MRA data from the same follow-up session. Two neurosurgeons independently compared the aneurysm occlusion status and flow visualization score in the stented parent artery (4-point scale, where 4 points represented excellent visualization) between TOF- and PETRA-MRA images. If DSA was performed within 3 months before or after PETRA-MRA, the aneurysm assessment was compared between MRA and DSA. The interobserver agreement for each MRA was evaluated.

**Results:** Nine of the 12 patients underwent DSA within 3 months before and after TOF- and PETRA-MRA. The aneurysm occlusion status on DSA was more consistent with PETRA-MRA (eight of nine cases) than with TOF-MRA (one of nine cases;  $P = 0.023$ ). The median visualization score of the stented parent artery was significantly higher for PETRA-MRA (4 [interquartile range {IQR} 3–4]) than for TOF-MRA (1 [IQR 1–1],  $P = 0.003$ ). The interobserver agreement for evaluation of the aneurysm occlusion status and visualization score of the parent artery for PETRA-MRA were excellent ( $\kappa = 0.98$  and  $0.93$ , respectively). In one case, PETRA-MRA was able to detect aneurysm recurrence, leading to subsequent retreatment.

**Conclusion:** PETRA-MRA is a noninvasive examination that can be used to evaluate the occlusion status of aneurysms after SAC and visualize the stented parent artery. PETRA-MRA is useful for repeated follow-up examinations after SAC.

**Keywords** ► PETRA-MRA, stent-assisted coil embolization, cerebral aneurysm, follow-up imaging

## Introduction

Regular follow-up imaging is necessary to assess recanalization after coil embolization of cerebral aneurysms. Follow-up imaging after coil embolization can often be

*Department of Neurosurgery, Suiseikai Kajikawa Hospital, Hiroshima, Hiroshima, Japan*

Received: April 7, 2023; Accepted: June 19, 2023

Corresponding author: Yusuke Ebiko. Department of Neurosurgery, Suiseikai Kajikawa Hospital, 1-1-23, Higashisenda-machi, Naka-ku, Hiroshima, Hiroshima 730-0053, Japan

Email: [sidebiko@gmail.com](mailto:sidebiko@gmail.com)



This work is licensed under a Creative Commons Attribution-NonCommercial-NoDerivatives International License.

©2023 The Japanese Society for Neuroendovascular Therapy

evaluated using time-of-flight (TOF) MRA; however, in the case of stent-assisted coil embolization (SAC), evaluation using TOF-MRA is difficult because of metal artifacts caused by the stent. DSA is the gold standard for follow-up imaging after SAC; however, there are risks of side effects from contrast media, radiation exposure, and procedural complications.

Pointwise encoding time reduction with radial acquisition (PETRA)-MRA is a noninvasive imaging method characterized by an ultrashort echo time (TE) and has been attracting attention in recent years because it considerably reduces metal artifacts.<sup>1-3)</sup> PETRA-MRA has the potential for postoperative evaluation of aneurysms and visualization of blood flow in stents. Therefore, this study aimed to evaluate the effectiveness of PETRA-MRA for follow-up imaging after SAC.

## Materials and Methods

### Patient selection

This retrospective study evaluated 12 patients (8 women and 4 men; mean age,  $66.9 \pm 13.2$  years) who underwent SAC for unruptured aneurysms at our hospital between April 2012 and June 2022. All patients underwent TOF- and PETRA-MRA during the same follow-up period. This retrospective study protocol was approved by the Institutional Review Board of Suisaikai Kajikawa Hospital. The requirement for informed consent from all participants was waived owing to the retrospective study design.

### Imaging acquisition

TOF- and PETRA-MRA were performed in a single-scan session using a 1.5-T MR scanner (AVANTO; Siemens Healthcare, Erlangen, Germany) with a 128-channel head-neck coil. The scan parameters for TOF-MRA were as follows: repetition time (TR)/TE, 26.0/7.15 ms; flip angle, 20°; field of view (FOV), 160 × 160 mm; matrix, 384 × 307; voxel size, 0.5 × 0.5 × 0.5 mm<sup>3</sup>; section thickness, 0.5 mm; compressed sensing factors, 9; bandwidth, 125 Hz/pixel; acquisition time, 8 min 50 s; and the number of slabs, 5. PETRA-MRA used the following scan parameters: TR/TE, 3.32/0.07 ms; flip angle, 6°; FOV, 280 × 280 mm; matrix, 320 × 320; radial sampling, 60,000 radial spokes; voxel size, 0.88 × 0.88 × 0.88 mm<sup>3</sup>; section thickness, 0.88 mm; and bandwidth, 400 Hz/pixel. Because PETRA-MRA was subtracted from the two imaging sets with and without a slice-selective saturation slab at the bottom of the imaging volume, the total acquisition time for PETRA-MRA was 9 min 16 s for data with or without a saturation band. DSA images were acquired using an Allura Clarity FD20/15 (Phillips Healthcare, Best, Netherlands).

### Image analysis

In each case, PETRA- and TOF-MRA performed simultaneously were evaluated and compared for the presence or absence of a residual aneurysm or recurrence and visualization of flow in the stented parent artery. If DSA was performed within 3 months before or after PETRA-MRA, the aneurysm assessment was compared between PETRA-MRA and DSA. If PETRA-MRA was performed multiple times in the same patient, imaging performed at the same time as DSA or the most recent imaging if DSA was not performed was evaluated.

Persistent or recurrent aneurysms were evaluated using maximum intensity projection (MIP) images for PETRA- and TOF-MRA and volume rendering (VR) and MIP images for DSA. Aneurysm size and parent artery diameter were measured using VR and MIP images for DSA. Aneurysm size was defined as the maximum diameter of the aneurysm. Parent artery diameter was defined as the mean diameter immediately proximal and distal to the aneurysm neck.

The above evaluations were performed independently by two neurosurgeons, and cases with different evaluations were discussed to reach the final evaluation. The presence or absence of residual or recurrent aneurysms was classified as complete occlusion (CO), neck remnant (NR), or body filling. Aneurysms that could not be evaluated owing to missing parent artery visualization were considered unevaluable (UE). Visualization of flow in the stented parent artery was scored as previously described by Irie et al.<sup>4</sup>: 1, not visible (almost no signal in the stent); 2, poor (structures are slightly visible but with significant blurring or artifacts, not diagnostic); 3, good (good-quality diagnostic information with minimal blurring or artifacts); and 4, excellent (excellent-quality diagnostic information; the shape of depiction is nearly equal to that of the DSA). For scores <2, evaluation of the aneurysm occlusion status was judged to be difficult.

### Statistical analyses

Continuous variables are presented as mean ± standard deviation. We compared whether the assessment of aneurysm occlusion status on DSA was consistent with that on TOF- and PETRA-MRA using the McNemar's test. The flow visualization scores of the stented parent artery for each MRA were compared using the Wilcoxon signed-rank test. A *P* value <0.05 was considered statistically significant. Interobserver agreement between the two readers was calculated using weighted κ coefficients and interpreted as follows: poor (<0.20), fair (0.21–0.40), moderate (0.41–0.60), good (0.61–0.80), or excellent (0.81–1.00).

All statistical analyses were performed using EZR version 1.52 (Saitama Medical Center, Jichi Medical University, Saitama, Japan), a graphical user interface for R version 4.02 (The R Foundation for Statistical Computing, Vienna, Austria). More precisely, it is a modified version of the R commander designed to add statistical functions frequently used in biostatistics.<sup>5</sup>

## Results

The mean size of the analyzed aneurysms and diameter of the parent artery were  $7.3 \pm 3.0$  mm and  $2.9 \pm 0.7$  mm, respectively (**Table 1**). The aneurysm was located in the internal carotid artery (ICA)–posterior communicating artery (Pcom) in three patients, paraclinoid segment of the ICA in two, ICA terminal in one, and anterior communicating artery (Acom) in six. The stents used were the Neuroform Atlas (Stryker, Kalamazoo, MI, USA) in eight patients, Enterprise2 VRD (Johnson & Johnson, Raynham, Miami, FL, USA) in one, LVIS Blue (MicroVention Inc., Aliso Viejo, CA, USA) in one, and LVIS Jr. (MicroVention Inc.) in two. None of the patients had more than one stent deployed. Five patients underwent coil embolization of the same aneurysm prior to SAC. Two patients had a history of aneurysmal neck clipping for other aneurysms prior to SAC.

DSA was performed within 3 months before and after TOF and PETRA-MRA in nine patients (**Table 2**). The time interval between TOF/PETRA-MRA and DSA was 28 days in one case and 1 day in the other eight cases. Flow visualization in the stented parent artery was defective on TOF-MRA in 10 of the 12 patients; therefore, evaluation of the aneurysm occlusion status was difficult in these cases. In contrast, PETRA-MRA allowed the assessment of the aneurysm occlusion status in all but one case. Enterprise2 VRD stent was used in the only case in which the aneurysm occlusion status was difficult to evaluate on PETRA-MRA. When comparing the flow visualization score in the stented artery on PETRA-MRA according to the type of stent, seven cases with the Neuroform Atlas scored 4 points and one case 3 points, one case with the LVIS Blue scored 3 points, two cases with the LVIS Jr. scored 4 points, and one case with the Enterprise2 VRD scored 1 point. Visualization of the stented parent artery was good in most cases with the Neuroform Atlas and LVIS Jr. and slightly weaker in one case with the LVIS Blue.

In the evaluation of aneurysm occlusion status, DSA and PETRA-MRA were consistent in eight of nine cases, while DSA and TOF-MRA were consistent in only one case, showing a significant difference ( $P = 0.023$ , McNemar's test). The only case in which DSA and PETRA-MRA evaluations differed was Case No. 10. DSA evaluation showed a slight NR of approximately 1 mm, whereas PETRA-MRA evaluation was CO. The NR of approximately 1 mm detected using DSA was not detected

**Table 1** Patient characteristics

| Characteristic                                    | Total $n = 12$  |
|---|-----------------|
| Age (years, mean $\pm$ SD)                        | $66.9 \pm 13.2$ |
| Gender ( $n$ , male/female)                       | 4/8             |
| Location of aneurysm ( $n$ )                      |                 |
| ICA–Pcom  | 3               |
| ICA C2  | 2               |
| ICA top   | 1               |
| Acom  | 6               |
| Size of aneurysm (mm, mean $\pm$ SD)              | $7.3 \pm 3.0$   |
| Diameter of parent artery (mm, mean $\pm$ SD)     | $2.9 \pm 0.7$   |
| Stent type ( $n$ )                                |                 |
| Enterprise2 VRD                                   | 1               |
| Neuroform Atlas                                   | 8               |
| LVIS Blue   | 1               |
| LVIS Jr.  | 2               |
| History of coil embolization prior to SAC ( $n$ ) | 5               |
| History of other aneurysm treatments ( $n$ )      | 2               |
| History of aneurysmal clipping ( $n$ )            | 2               |

Acom: anterior communicating artery; ICA: internal carotid artery; Pcom: posterior communicating artery; SAC: stent-assisted coil embolization

using PETRA-MRA. The median visualization score of the parent artery using TOF-MRA was 1 (interquartile range [IQR] 1–1), and the median score using PETRA-MRA was 4 (IQR 3–4), showing a significant difference ( $P = 0.003$ , Wilcoxon signed-rank test). The interobserver agreement for evaluation of the aneurysm occlusion status and visualization score of the parent artery for PETRA-MRA were both excellent ( $\kappa = 0.98$  and  $0.93$ , respectively).

### Representative cases

#### 1. Case No. 2

A 79-year-old woman developed a subarachnoid hemorrhage (SAH) 28 years prior to presentation and underwent neck clipping for a right ICA–Pcom aneurysm. Sixteen years later, coil embolization was performed for the unruptured left ICA–Pcom aneurysm (**Fig. 1A**). However, 2 years later, the aneurysm recurred and SAC was performed (**Fig. 1B–1D**). An Enterprise2 VRD  $4.5 \times 28$  mm stent was deployed in the left ICA (**Fig. 1C**). PETRA-MRA performed 10 years after the SAC (**Fig. 1F**) lacked visualization of the stented parent artery, similar to TOF-MRA (**Fig. 1E**), which made it difficult to evaluate the aneurysm occlusion status.

#### 2. Case No. 7

A 76-year-old woman developed an SAH 6 years ago and underwent coil embolization for a right ICA–Pcom aneurysm. Five years later, she developed a recurrent aneurysm

**Table 2 TOF/PETRA MRA and DSA assessment of all patients**

| Case No. | Aneurysm location | Stent/length (mm)         | Parent artery diameter (mm) | Aneurysm occlusion status |       |     | Visualization score of the flow in the stent |       | Interval from SAC |           |
|----------|-------------------|---------------------------|-----------------------------|---------------------------|-------|-----|--|-------|-------------------|-----------|
|          |                   |                           |                             | TOF                       | PETRA | DSA | TOF  | PETRA | to DSA            | to MRA    |
| 1        | Acom              | Neuroform Atlas/ 3.0 × 21 | 2.4                         | UE                        | BF    | N/A | 1  | 4     | N/A               | 18 months |
| 2        | ICA-Pcom          | Enterprise2 VRD/ 4.5 × 28 | 3.7                         | UE                        | UE    | N/A | 1  | 1     | N/A               | 10 years  |
| 3        | Acom              | Neuroform Atlas/ 3.0 × 21 | 2.6                         | UE                        | NR    | NR  | 1  | 4     | 0 day             | 1 day     |
| 4        | ICA-Pcom          | Neuroform Atlas/ 4.5 × 30 | 3.8                         | UE                        | CO    | N/A | 1  | 3     | N/A               | 5 years   |
| 5        | Acom              | LVIS Jr./3.5 × 18         | 3                           | UE                        | CO    | CO  | 1  | 4     | 1 year            | 1 year    |
| 6        | Acom              | LVIS Jr./2.5 × 17         | 2                           | UE                        | NR    | NR  | 1  | 4     | 3 months          | 2 months  |
| 7        | ICA-Pcom          | Neuroform Atlas/ 4.0 × 21 | 3.2                         | UE                        | NR    | NR  | 1  | 4     | 0 day             | 1 day     |
| 8        | ICA top           | Neuroform Atlas/ 4.5 × 30 | N/A                         | NR                        | BF    | BF  | 2  | 4     | 0 day             | 1 day     |
| 9        | Acom              | Neuroform Atlas/ 3.0 × 21 | 2.2                         | UE                        | NR    | NR  | 1  | 4     | 0 day             | 1 day     |
| 10       | Acom              | Neuroform Atlas/ 3.0 × 21 | 2.2                         | UE                        | CO    | NR  | 1  | 4     | 0 day             | 1 day     |
| 11       | ICA C2            | Neuroform Atlas/ 4.0 × 21 | 3.2                         | NR                        | NR    | NR  | 2  | 4     | 0 day             | 1 day     |
| 12       | ICA C2            | LVIS Blue/ 4.5 × 18       | 4                           | UE                        | NR    | NR  | 1  | 3     | 0 day             | 1 day     |

Visualization score of the flow in stent: 1, not visible (almost no signal in the stent); 2, poor (structures are slightly visible but with significant blurring or artifacts, not diagnostic); 3, good (good-quality diagnostic information with minimal blurring or artifacts); 4, excellent (excellent-quality diagnostic information; the shape of depiction is nearly equal to that of DSA). Acom: anterior communicating artery; BF: body filling; CO: complete occlusion; ICA: internal carotid artery; N/A: not available; NR: neck remnant; Pcom: posterior communicating artery; PETRA: pointwise encoding time reduction with radial acquisition; SAC: stent-assisted coil embolization; TOF: time-of-flight; UE: unevaluable

(**Fig. 2A**) and SAC was performed (**Fig. 2B–2D**). A Neuroform Atlas 4.0 × 21 mm stent was deployed from the Pcom to the ICA (**Fig. 2C**). TOF-MRA performed on the day after SAC revealed a defect in the stented parent artery, making it difficult to evaluate the occlusion status of the aneurysm (**Fig. 2E**). Conversely, PETRA-MRA showed good visualization of the stented parent artery, and the aneurysm occlusion status was evaluated as CO (**Fig. 2F**). TOF-MRA performed 3 months after SAC revealed a faint high intensity within the aneurysm and defect in the origin of the Pcom (**Fig. 2G**). PETRA-MRA performed on the same day revealed aneurysm recurrence and a stented parent artery (**Fig. 2H**). After reconfirmation using DSA (**Fig. 2I**), additional coil embolization was performed (**Fig. 2J**). PETRA-MRA was performed the day after assessing the aneurysm occlusion status as NR (**Fig. 2K**).

### 3. Case No. 9

A 56-year-old woman underwent SAC for an unruptured Acom aneurysm with a maximum diameter of 6.7 mm

(**Fig. 3A**). A Neuroform Atlas 3.0 × 21 mm stent was deployed from the left A2 to A1 (**Fig. 3C**). The final angiography performed during SAC revealed an NR of the aneurysm (**Fig. 3D**). TOF-MRA performed on the day after SAC showed that the parent artery and aneurysm were defective, making it difficult to evaluate the occlusion status (**Fig. 3E**). However, PETRA-MRA depicted the NR of the aneurysm, which was consistent with the DSA findings during SAC (**Fig. 3F**).

## Discussion

The recurrence rate after coil embolization of cerebral aneurysms is reported to be 27.9%, which decreases to 12.7% in cases of SAC.<sup>6)</sup> However, the recurrence rate cannot be ignored, and regular postoperative follow-up imaging is necessary. TOF-MRA is often used to screen for postoperative recurrence of coil embolization without stenting. However, in the case of SAC, evaluation using TOF-MRA is often difficult because of metal artifacts

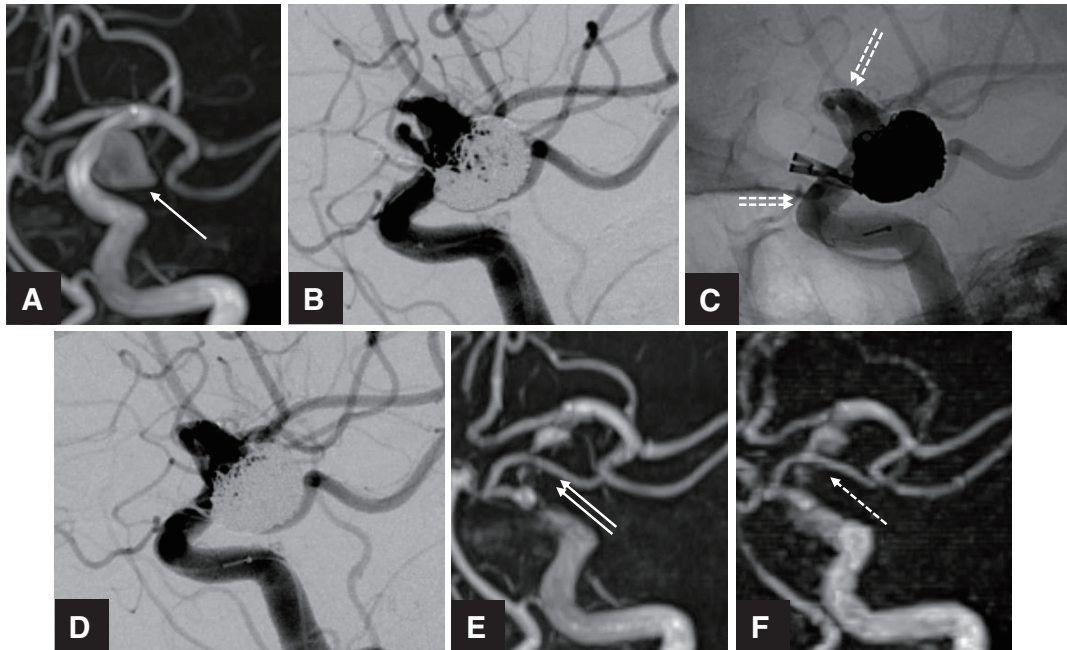


**Fig. 1** The patient developed SAH and underwent neck clipping of the right ICA–Pcom aneurysm. (A) TOF-MRA performed 16 years after the SAH showing an unruptured left ICA–Pcom aneurysm (white arrow). Coil embolization of the aneurysm was performed. (B) Left internal carotid angiography performed 2 years after coil embolization showing aneurysmal recurrence. (C) SAC was performed to treat aneurysm recurrence. An Enterprise2 VRD stent measuring 4.5 × 28 mm was deployed in the left ICA. Double white dotted arrows indicate the proximal and distal markers of the stent. (D) Left internal carotid angiography after SAC. (E) TOF-MRA performed 10 years after SAC showing a defect in the left ICA around the aneurysm, making it difficult to evaluate the occlusion status of the aneurysm (double white arrows). (F) PETRA-MRA performed on the same day as TOF-MRA showing a defect in the stented parent artery (white dotted arrow). ICA: internal carotid artery; ICA–Pcom: internal carotid artery-posterior communicating artery; PETRA: pointwise encoding time reduction with radial acquisition; SAC: stent-assisted coil embolization; SAH: subarachnoid hemorrhage; TOF: time of flight



**Fig. 2** The patient developed SAH, and coil embolization of the right ICA–Pcom aneurysm was performed. (A) TOF-MRA performed 6 years after coil embolization showing aneurysmal recurrence (white arrow). (B–D) Working views of the right internal carotid angiography before (B) and after SAC (D). A Neuroform Atlas stent measuring 4.0 × 21 mm was deployed from the right Pcom to the right ICA (C). Black arrows indicate the proximal and distal markers of the stent. (E) TOF-MRA on the day after SAC showing a defect in the parent artery around the aneurysm (double white arrows). (F) PETRA-MRA on the same day showing the stented parent artery, and the aneurysm was not visualized (white dotted arrow). (G) TOF-MRA performed 3 months after SAC showing a faint high intensity

within the aneurysm (double white dotted arrows) and defect in the origin of Pcom. (H) PETRA-MRA performed on the same day showing the NR of the aneurysm (triple white arrows) and stented parent artery. (I and J) After confirming similar findings on DSA (I), additional coil embolization was performed (J). (K) PETRA-MRA was performed the day after assessing the aneurysm as NR (triple white dotted arrows). ICA: internal carotid artery; ICA–Pcom: internal carotid artery–posterior communicating artery; NR: neck remnant; Pcom: posterior communicating artery; PETRA: pointwise encoding time reduction with radial acquisition; SAC: stent-assisted coil embolization; SAH: subarachnoid hemorrhage; TOF: time of flight

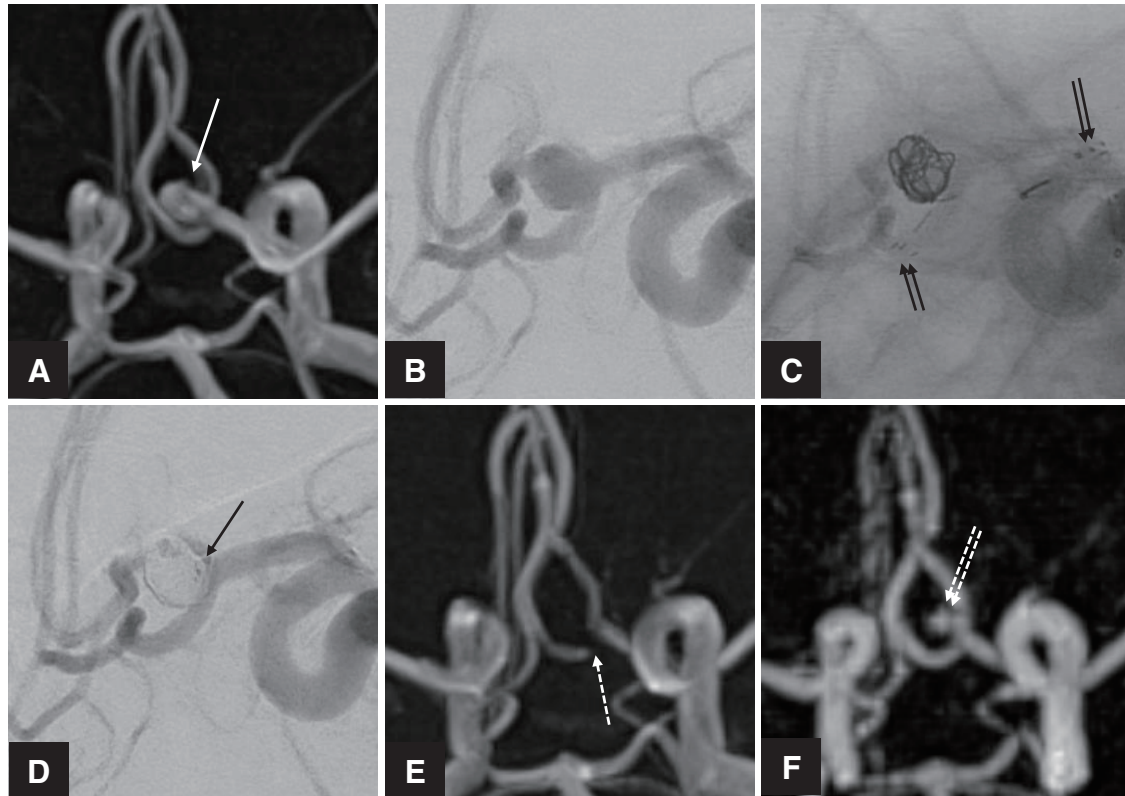


**Fig. 3** (A) Preoperative TOF-MRA showing Acom (left A1–A2) aneurysm (white arrow). (B) Working view on left internal carotid angiography before SAC. (C) A Neuroform Atlas stent measuring  $3.0 \times 21$  mm was deployed from left A2 to left A1. Double black arrows indicate the proximal and distal markers of the stent. (D) Working view on left ICA after SAC showing the NR of the aneurysm (black arrow). (E) TOF-MRA on the day after SAC showing a defect in the parent artery around the aneurysm (white dotted arrow). (F) PETRA-MRA on the same day showing the NR of the aneurysm (double white dotted arrows). Acom: anterior communicating artery; NR: neck remnant; PETRA: pointwise encoding time reduction with radial acquisition; SAC: stent-assisted coil embolization; TOF: time of flight

caused by the stent. After aneurysm clipping, CTA can often be used for evaluation. However, in the case of SAC, it is difficult to evaluate using CTA, as with TOF-MRA, because of metal artifacts of the coils and stents. Therefore, DSA has been regarded as the gold standard for evaluation after SAC. However, DSA is an invasive examination and is associated with a risk of complications, such as side effects from contrast media and cerebral infarction due to catheter manipulation.

PETRA-MRA is a noninvasive imaging method characterized by an ultrashort TE, which is commercially available in Siemens MRI equipment. It has attracted significant attention in recent years because of its ability to significantly reduce metal artifacts.<sup>1–3)</sup> In this study, the aneurysm occlusion status was evaluated using PETRA-MRA in 11 of the 12 patients after SAC. In nine cases, PETRA-MRA and DSA findings were compared. In eight of the nine cases, the assessment of aneurysm occlusion status using PETRA-MRA and DSA was consistent.

Therefore, postoperative evaluation of the SAC using PETRA-MRA is possible in most cases. Conversely, TOF-MRA lacks the visualization of the stented parent artery in most cases, making it difficult to evaluate the occlusion status of the aneurysm.

In one case where an Enterprise2 VRD stent was placed, the PETRA-MRA aneurysm occlusion status was judged to be UE. In this case, PETRA-MRA, similar to TOF-MRA, lacked visualization of the stented parent artery, making aneurysm evaluation difficult. Heo et al.<sup>7)</sup> reported that visualization of the stented parent artery was better with the Neuroform stent than with the Enterprise stent, which is similar to the results of this study. This study also included cases that used LVIS Blue and LVIS Jr. stents where evaluating the occlusion status of aneurysms was possible. However, in cases where LVIS Blue was used, the visualization of the stented parent artery was slightly weaker (visualization score: 3) than in the two cases where LVIS Jr. was used (visualization score: 4). The parent

artery diameter was 4 mm in the case in which LVIS Blue was used, which was larger than that of the two LVIS Jr. cases (2 and 3 mm); however, the signal of the stented parent artery was slightly weaker. Thus, it is conceivable that the signal of the stented parent artery is affected by the type of stent, and it is speculated that one of the factors is that the metal density of the mesh is higher in LVIS Blue than in LVIS Jr. Possible causes of the difference in rendering by stents include stent design (open or closed cell), stent thickness, the amount and density of metal used, and the material used. Further investigation is required to examine these causes. In contrast, in this study, three patients had a visualization score of 3 points or less. All three stents were of different types but all had a diameter of 4.5 mm, which was the largest among the stents used in this study. It is possible that when a large-diameter stent is placed in the parent artery, the metal density of the mesh increases, making observation using PETRA-MRA difficult. However, this was difficult to evaluate owing to the small number of cases. Additionally, in these three cases, the curvature of the stented parent artery was not particularly strong, and it is unlikely that the curvature of the parent artery made it difficult to observe with PETRA-MRA.

In cases where the PETRA-MRA and DSA evaluations of the aneurysm occlusion status did not match (Case No. 10), DSA showed an NR of approximately 1 mm, whereas the PETRA-MRA evaluation was CO. PETRA-MRA may not detect NRs that are  $\leq 1$  mm in size. However, in this case, DSA during SAC and PETRA-MRA on the next day were compared; therefore, it is possible that the effects of postoperative heparin wear off and NRs were thrombosed, leading to CO the next day.

Consistent with the results of this study, Sato et al.<sup>8)</sup> reported the effectiveness of PETRA-MRA for image evaluation after SAC. Furthermore, they speculated that visualization of the stented parent artery might be obscured in cases with small-diameter vessels. In this study, the diameter of the smallest parent artery was 2.0 mm, and it was not possible to consider parent artery  $< 2.0$  mm in diameter.

In the representative case 2, recurrence after SAC was detected using PETRA-MRA, which was subsequently retreated. To the best of our knowledge, this is the first report of such a case.

Similar to PETRA-MRA, Silent MRA, which is commercially available in GE Healthcare (Milwaukee, WI, USA) MRI equipment, has attracted attention in recent years as an imaging method that is characterized by an

ultrashort TE and can reduce magnetic susceptibility artifacts.<sup>4,9-11)</sup> Silent MRA, such as PETRA-MRA, is an imaging method that can reduce artifacts caused by metals, such as stents and coils. In Silent MRA, the blood vessels are visualized by subtracting the images before and after using the arterial spin-labeling technique. However, in PETRA-MRA, blood vessels are visualized by subtracting the image in which the inflow effect is removed by adding a saturation pulse to the blood-inflow region from the image obtained by the normal PETRA method, including the inflow effect.

While some studies have reported the usefulness of PETRA-MRA in follow-up after aneurysmal clipping,<sup>12,13)</sup> those that do so after SAC are rare. In addition to SAC, conditions that are difficult to evaluate postoperatively without DSA include cases after flow-diverter stenting and those in which clipping and coil embolization have been performed on the same aneurysm. Further studies are required to evaluate the usefulness of PETRA-MRA in the postoperative follow-up of such cases.

PETRA-MRA is a noninvasive examination; however, it has some disadvantages. First, the resolution is low, and consequently, it is possible that an NR of approximately 1 mm may not be detected. In addition, the evaluation of blood vessel diameters is difficult. Second, the acquisition time is relatively long (approximately 10 min) as it requires subtraction, and evaluable images could not be obtained in patients who moved during the examination. However, despite these disadvantages, this noninvasive examination is effective for repeated postoperative follow-ups.

This study had several limitations. First, its retrospective design was prone to selection bias. Second, the number of patients included in this study was small. Third, there were no patients with posterior circulation aneurysms. Fourth, in seven of the nine patients who could be compared using both PETRA-MRA and DSA, DSA was assessed during SAC and PETRA-MRA was assessed the next day. Thus, there is a possibility that the occlusion status may have changed due to postoperative thrombosis of the aneurysm between the SAC and PETRA-MRA.

## Conclusion

PETRA-MRA is a noninvasive examination that can be used to evaluate the occlusion status of aneurysms after SAC and visualize the stented parent artery. Therefore, PETRA-MRA may be useful as a repeated examination during follow-up after SAC.

## Disclosure Statement

The authors have no conflicts of interest to declare.

## References

- 1) You SH, Kim B, Yang KS, et al. Ultrashort echo time magnetic resonance angiography in follow-up of intracranial aneurysms treated with endovascular coiling: comparison of time-of-flight, pointwise encoding time reduction with radial acquisition, and contrast-enhanced magnetic resonance angiography. *Neurosurgery* 2021; 88: E179–E189.
- 2) Zhang F, Ran Y, Zhu M, et al. The use of pointwise encoding time reduction with radial acquisition MRA to assess middle cerebral artery stenosis pre- and post-stent angioplasty: comparison with 3D time-of-flight MRA and DSA. *Front Cardiovasc Med* 2021; 8: 739332.
- 3) Katsuki M, Kakizawa Y, Yamamoto Y, et al. Magnetic resonance angiography with ultrashort echo time evaluates cerebral aneurysm with clip. *Surg Neurol Int* 2020; 11: 65.
- 4) Irie R, Suzuki M, Yamamoto N, et al. Assessing blood flow in an intracranial stent: a feasibility study of MR angiography using a silent scan after stent-assisted coil embolization for anterior circulation aneurysms. *AJNR Am J Neuroradiol* 2015; 36: 967–970.
- 5) Kanda Y. Investigation of the freely available easy-to-use software 'EZR' for medical statistics. *Bone Marrow Transplant* 2013; 48: 452–458.
- 6) Phan K, Huo YR, Jia F, et al. Meta-analysis of stent-assisted coiling versus coiling-only for the treatment of intracranial aneurysms. *J Clin Neurosci* 2016; 31: 15–22.
- 7) Heo YJ, Jeong HW, Baek JW, et al. Pointwise encoding time reduction with radial acquisition with subtraction-based MRA during the follow-up of stent-assisted coil embolization of anterior circulation aneurysms. *AJNR Am J Neuroradiol* 2019; 40: 815–819.
- 8) Sato K, Asano A, Kobayashi T, et al. Validity of PETRA-MRA for stent-assisted coil embolization of intracranial aneurysms. *JNET J Neuroendovasc Ther* 2021; 15: 352–359.
- 9) Takano N, Suzuki M, Irie R, et al. Non-contrast-enhanced silent scan MR angiography of intracranial anterior circulation aneurysms treated with a low-profile visualized intraluminal support device. *AJNR Am J Neuroradiol* 2017; 38: 1610–1616.
- 10) Takano N, Suzuki M, Irie R, et al. Usefulness of non-contrast-enhanced MR angiography using a silent scan for follow-up after Y-configuration stent-assisted coil embolization for basilar tip aneurysms. *AJNR Am J Neuroradiol* 2017; 38: 577–581.
- 11) Satoh T, Hishikawa T, Hiramatsu M, et al. Visualization of aneurysmal neck and dome after coiling with 3D multifusion imaging of silent MRA and FSE-MR cisternography. *AJNR Am J Neuroradiol* 2019; 40: 802–807.
- 12) Kim JH, Ahn SJ, Park M, et al. Follow-up imaging of clipped intracranial aneurysms with 3-T MRI: comparison between 3D time-of-flight MR angiography and pointwise encoding time reduction with radial acquisition subtraction-based MR angiography. *J Neurosurg* 2021; 136: 1260–1265.
- 13) Nishikawa A, Kakizawa Y, Wada N, et al. Usefulness of pointwise encoding time reduction with radial acquisition and subtraction-based magnetic resonance angiography after cerebral aneurysm clipping. *World Neurosurg X* 2021; 9: 100096.